Defect-Induced Photoluminescence Enhancement and Corresponding Transport Degradation in Individual Suspended Carbon Nanotubes

Bo Wang, Lang Shen, Sisi Yang, Jihan Chen, Juliana Echternach, Rohan Dhall, DaeJin Kang, and Stephen Cronin

Phys. Rev. Applied **9**, 054022 — Published 16 May 2018

DOI: 10.1103/PhysRevApplied.9.054022

Defect-induced Photoluminescence Enhancement and Corresponding Transport Degradation in Individual Suspended Carbon Nanotubes

Bo Wang[1], Lang Shen[2], Sisi Yang[1], Jihan Chen[3], Juliana Echternach[3], Rohan Dhall[3], Daejin Kang[4], and Stephen Cronin[1, 3]

[1]Department of Physics and Astronomy, [2]Mork Family Department of Chemical Engineering and Material Science, [3]Ming Hsieh Department of Electrical Engineering, University of Southern California, Los Angeles, CA 90089, USA`

[4]Department of Mechatronics Engineering, Korea Polytechnic University, Siheung, Gyeonggi 15073, Republic of Korea

Abstract

The utilization of defects in carbon nanotubes to improve their photoluminescence efficiency has become a widespread study towards the realization of efficient light emitting devices. Here, we report a detailed comparison of defects in nanotubes (quantified by Raman spectroscopy) and photoluminescence (PL) intensity of individual suspended carbon nanotubes (CNTs). We have also the evaluated the impact of these defects on the electron/hole transport in the nanotubes, which is crucial for the ultimate realization of optoelectronic devices. We find that brightly luminescent nanotubes exhibit a pronounced D-band in their Raman spectra, and vice versa, dimly luminescent nanotubes exhibit almost no D-band. Here, defects are advantageous for light emission by trapping excitons, which extends their lifetimes. We quantify this behavior by plotting the PL intensity as a function of the D/G band Raman intensity ratio, which exhibits a Lorentz distribution peaked at D/G=0.17. For CNTs with a D/G ratio >0.25, the PL intensity decreases, indicating that, above some critical density, non-radiative recombination at defect sites dominates over the advantages of exciton trapping. In an attempt to fabricate

optoelectronic devices based on these brightly luminescent CNTs, we transferred these suspended CNTs to platinum electrodes and found that the brightly photoluminescent nanotubes exhibit nearly infinite resistance due to these defects while those without bright photoluminescence exhibit finite resistance. These findings indicate a potential limitation in the use of brightly luminescent CNTs for optoelectronic applications.

Keywords: carbon nanotube, CNT, photoluminescence, defects, quenching, luminescence

I. INTRODUCTION

Enhanced photoluminescence in carbon nanotubes and 2D materials due to defect-localized exciton states has been reported by several research groups over the past few years.[1-11] This work typically requires defects to be created through some form of post-growth treatment. For example, oxygen doping of carbon nanotubes (CNTs) through ozonolysis has been shown to produce localized exciton states that exhibit enhanced photoluminescence intensities (~20X), long photoluminescence lifetimes (>1nsec), and single photon emission, even at room temperature.[12-15] These oxygen dopant sites in carbon nanotubes are well understood with a detailed atomic scale picture based on DFT calculations, and robust methods exist for creating these defect/dopant sites. UV/ozone treatment of air-suspended CNTs has also been shown to provide up to 5-fold enhancements in the PL intensity by the creation of such defects. While there have been many purely optical studies of CNTs, studies of optoelectronic phenomena are relatively few.[16-20] Also, a vast majority of previous carbon nanotube studies were performed on large ensembles of nanotubes rather than individual CNTs.

In the work presented here, we correlate the defect density in as-grown CNTs with their PL intensity without requiring the need for any post-growth processing. Previous studies were carried out on ensembles of nanotubes and, thus, it was not possible to obtain a 1-to-1 correlation between the PL intensity and the D-band Raman mode, which provides a relative measure of the amount of defects in carbon nanotubes.[21-23] Here, we study air-suspended CNTs rather than surfactant-suspended CNTs. The electrical resistance is used to further characterize the nature of these defects and the extent to which they perturb the electron and hole transport in this system.

II. EXPERIMENTAL SETUP AND METHOD

Samples are fabricated by etching 8μm deep, 2μm × 2μm pillars in a quartz substrate using a Cl-based reactive ion etch plasma. Optical and electron microscopy images of these pillars are shown in Figure 1. Before etching, a 1nm-thick film of Fe is deposited by electron beam evaporation to serve as a catalyst for the nanotube growth. Carbon nanotubes are grown by chemical vapor deposition (CVD) using ethanol as the carbon feedstock at 825^{o}C, as reported previously.[24, 25] Figure 1c shows a scanning electron microscope (SEM) image of CNTs suspended across these pillars grown using this technique. The PL related data is collected on a home built PL imaging system at room temperature, as shown in Figure 1(d). In this system, a 785 nm wavelength laser source (Spectra-Physics, Model 3900) is used to irradiate the sample. The illumination area is approximately 60μm in diameter. A 1100nm long pass filter is used to eliminate any Rayleigh or Raman scattered light. The PL signal is then collected with a thermoelectrically-cooled InGaAs camera (Xenics, Inc.), which is sensitive to IR light emission in the 1100-1600nm wavelength range. This IR camera is capable of outputing the light intensity for selected regions or individual pixels in the PL image. During these PL measurements, all the bright nanotubes of interest are moved to the same position relative to the center of the excitation area, and the PL intensity is obtained from the same pixel in order to minimize the variation between measurements. An optical microscope image of a 4 × 5 array of quartz pillars is shown in Figure 1a. Figure 1b shows a PL image taken from the same region of this sample. A bright line can be seen connecting two adjacent pillars, corresponding to PL emission from a suspended CNT. Raman spectra from these same individual suspended CNTs are collected using a Renishaw *InVia* micro-spectrometer. All Raman spectra are measured at room temperature using

a 785nm laser source with the same incident laser power, objective lens, grating, and integration time. Before collecting each Raman spectrum, several attempts are made to optimize the position and obtain the strongest Raman signal.

III. RESULTS AND DISCUSSION

Figure 2 shows the Raman spectra of 4 different suspended carbon nanotubes that exhibit dim photoluminescence. Figure 2a shows a representative photoluminescence image of one such dim nanotube. For all 4 nanotubes, the D-band is almost undetectable in these Raman spectra. The D/G band Raman intensity ratio for these nanotubes spans a range from 0 to 0.041.

Figure 3 shows the Raman spectra of 5 brightly photoluminescent CNTs, along with a representative PL image (Figure 3a). All of these Raman spectra exhibit pronounced D-bands, indicating the presence of a substantial amount of defects in these nanotubes. Here, the D/G band Raman intensity ratio spans a range from 0.075 to 0.16. Here, we believe that exciton localization at these defect sites prevents non-recombination that occurs at the ends of the CNT, ultimately extending their luminescence efficiencies and lifetimes. Interestingly, even though the defect-enhanced PL is provided by localized excitons (i.e., 0D system), these nanotubes appear as lines in the PL images, indicating that there are many such defects along the length of each nanotube. The spatial resolution of our PL imaging setup is around 0.5μm, as shown in Figure S1 in the Supplemental Document.

Figure 4 shows the Raman spectra of 4 nanotubes that exhibit D/G band Raman intensity ratios greater than 0.25. These highly defective nanotubes exhibit relatively dim photoluminescence. Here, we believe that non-radiative recombination at these defect sites outweighs the advantageous effects of exciton trapping created by these defect sites. It is also

possible that these nanotubes have more substantial types of defects, such as vacancies or 5-7 defects.

Figure 5 plots the PL intensity of 13 nanotubes as a function of the D/G band Raman intensity ratio. Here, the data exhibits a Lorentzian distribution peaked at D/G=0.17. The wide dynamic range of the PL, here spanning almost 2 orders of magnitude, is immediately apparent in this plot. For CNTs with D/G ratios < 0.15, the PL intensity increases with defect density due to exciton localization. However, for CNTs with D/G ratios > 0.25, the PL intensity decreases, indicating that, above some critical density, non-radiative recombination at defect sites dominates over the advantages of exciton localization.

In an attempt to fabricate optoelectronic devices based on these brightly luminescent nanotubes, we developed a flip-chip transfer process to transfer brightly photoluminescent nanotubes suspended across quartz pillars to pre-patterned metal electrodes (i.e., Pt) on a separate chip, as illustrated in Figure 6. In this process, the CNT-containing pillars are slowly brought into contact with the electrode chip using a home built contact aligner. The quartz substrate is then lifted off slowly using a *z*-axis micromanipulator, resulting in complete transfer of the desired nanotube to the metal electrodes, suspended over the trench. Figure 6d shows an optical microscope image of the two chips in contact during the transport process.

Figure 7a shows an SEM image of a suspended CNT that has been successfully transferred using this technique. Disappointingly, 11 out of 11 bright nanotubes that were successfully transferred to these electrodes showed an extremely high resistance (R>1GΩ) due to the defects associated with exciton trapping. It is worth mentioning that the one-dimensional nature of CNTs make them particularly susceptible to defects, since electrons can only scatter

backwards. Figure 7b shows the current-gate voltage (I-V_{gate}) characteristics of a non-bright nanotube that was transferred to these electrodes. Here, the suspended nanotube was first identified by SEM rather than PL imaging. The I-V_{gate} characteristics show field effect transistor behavior that is typical of a semiconducting nanotube with a weak gate. Here, the effect of the underlying silicon gate is weak because the electrodes are 8μm tall and, hence, the underlying silicon is relatively far away from the CNT channel. Nevertheless, at a gate voltage of V_{gate}=-4V, the suspended nanotube exhibits a resistance of 200kΩ, which is at least three orders of magnitude lower than that of the brightly photoluminescent nanotubes that were transferred to the same electrodes. This data indicates the strong role that these defects play in preventing electron/hole transport, which will likely limit practical applications in electronically-driven light emission from carbon nanotubes.

IV. SUMMARY

In conclusion, we have compared the Raman spectra and photoluminescence (PL) intensities of individual suspended carbon nanotubes (CNTs). We find that brightly luminescent nanotubes exhibit pronounced D-bands in their Raman spectra, whereas dimly luminescent nanotubes exhibit almost no D-band. The relative defect density is quantified using the D/G band Raman intensity ratio. By plotting the PL intensity as a function of the D/G band Raman intensity ratio, we observe a Lorentzian distribution peaked at D/G=0.17. CNTs with a D/G ratio above 0.25 show a decreased PL intensity, indicating the point beyond which defects cause non-radiative recombination rather than exciton trapping. When these brightly luminescent nanotubes are transferred to metal electrodes, their resistance is found to be infinite (R>1GΩ) because of the presence of these defects. However, non-luminescent CNTs exhibit finite resistance. These results indicate that there may be an inherent limitation in the ultimate realization of

optoelectronic devices with a tradeoff between luminescence efficiency and low resistance carrier transport.

The spatial resolution of our PL imaging setup is around 1μm and the resistance of a blank chip used in the flip-chip transfer technique is around 2GΩ, as shown in the **Supplemental Material**[26].

ACKNOWLEDGEMENTS

The authors would like to acknowledge support from the Northrop Grumman-Institute of Optical Nanomaterials and Nanophotonics (NG-ION^2) (B.W). This research was also supported by the Department of Energy DOE Award No. DE-FG02-07ER46376 (J.C.) and National Science Foundation NSF Award No. 1402906 (S.Y.). A portion of this work was carried out in the University of California Santa Barbara (UCSB) nanofabrication facility. The authors would also like to acknowledge the help from Daejin Kang of Korea Polytechnic University.

Figures

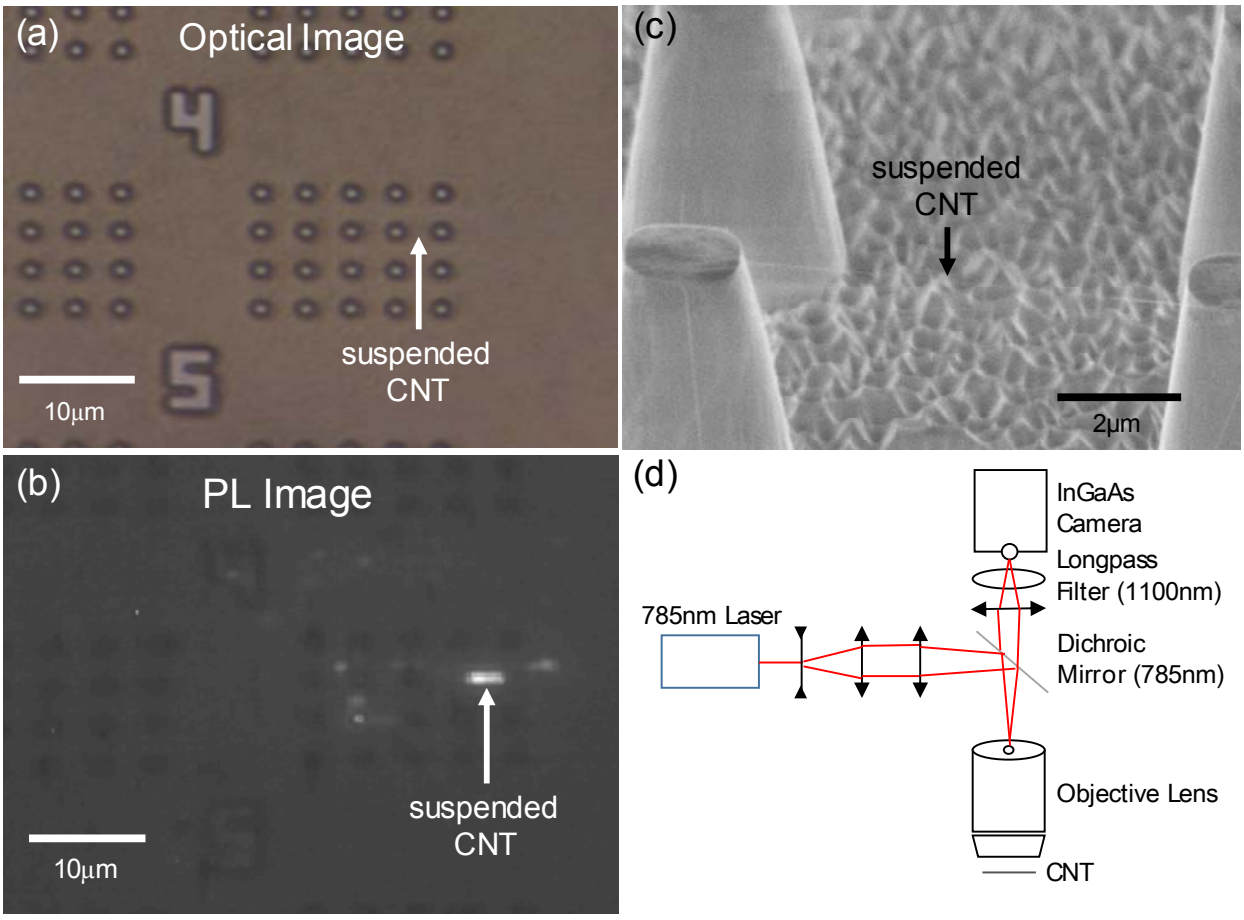

Figure 1. (a) Optical, (b) photoluminescence, and (c) SEM images of carbon nanotubes suspended across quartz pillars. (d) Schematic diagram of the photoluminescence imaging setup.

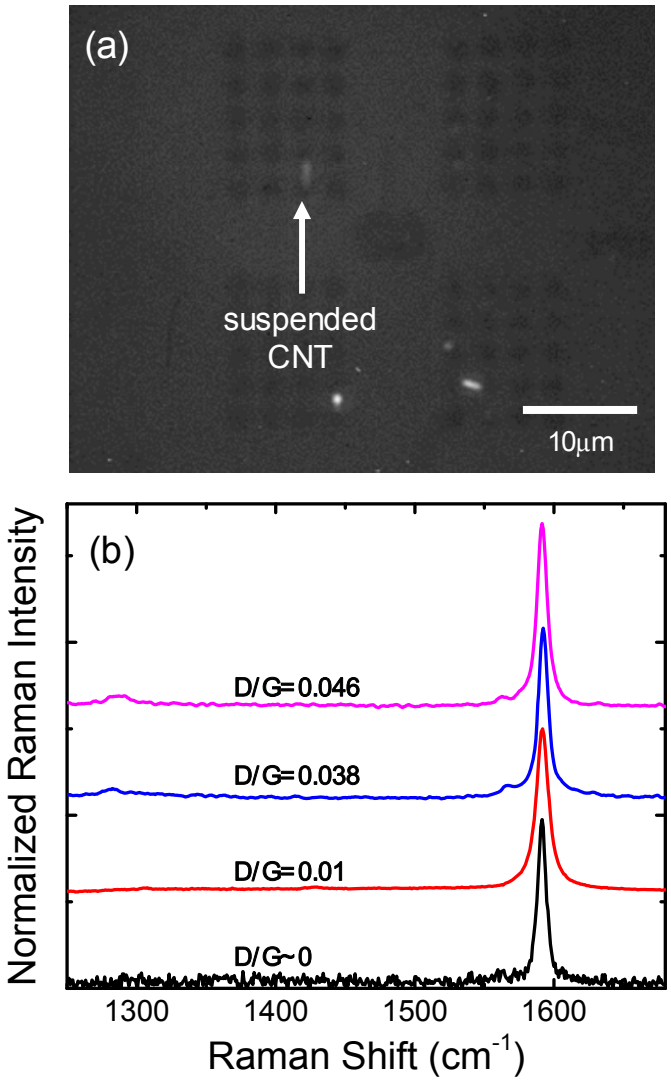

Figure 2. (b) Raman spectra of 4 different suspended carbon nanotubes that exhibit dim photoluminescence and (a) representative photoluminescence image.

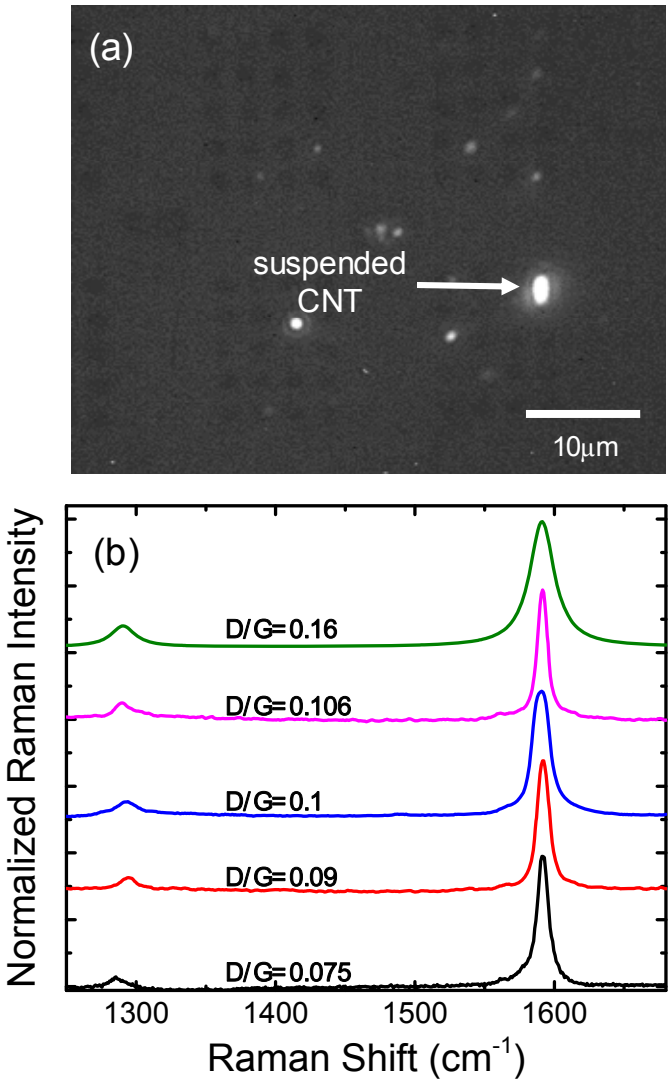

Figure 3. (b) Raman spectra of 5 different suspended carbon nanotubes that exhibit bright photoluminescence and (a) representative photoluminescence image.

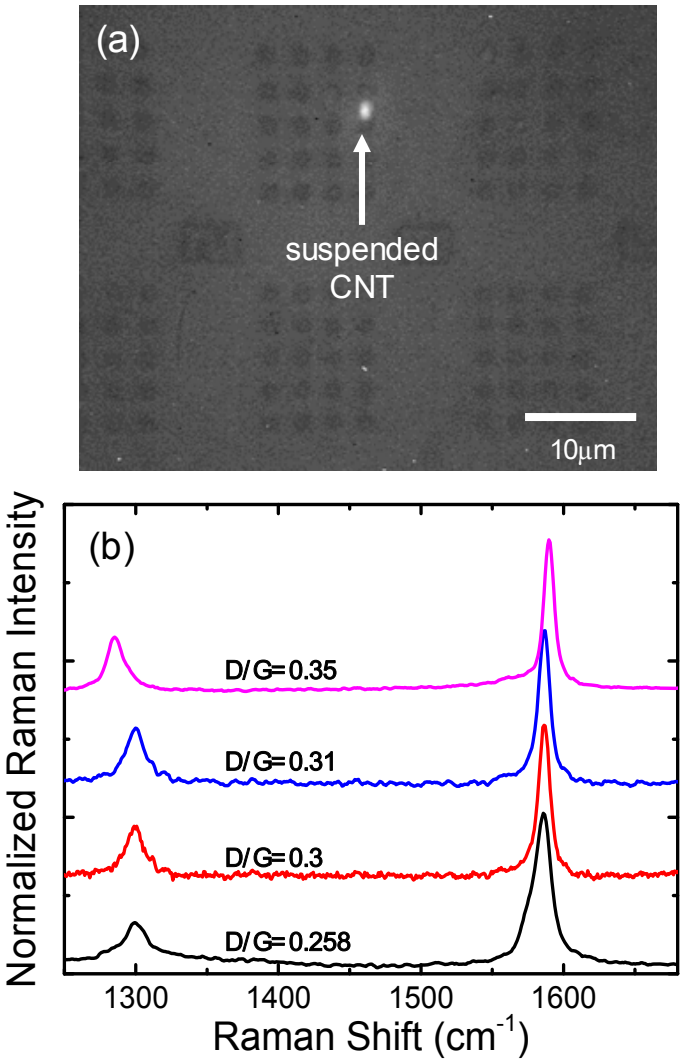

Figure 4. (a) Representative PL image and (b) Raman spectra of 4 different suspended carbon nanotubes that exhibit D/G ratios > 0.25.

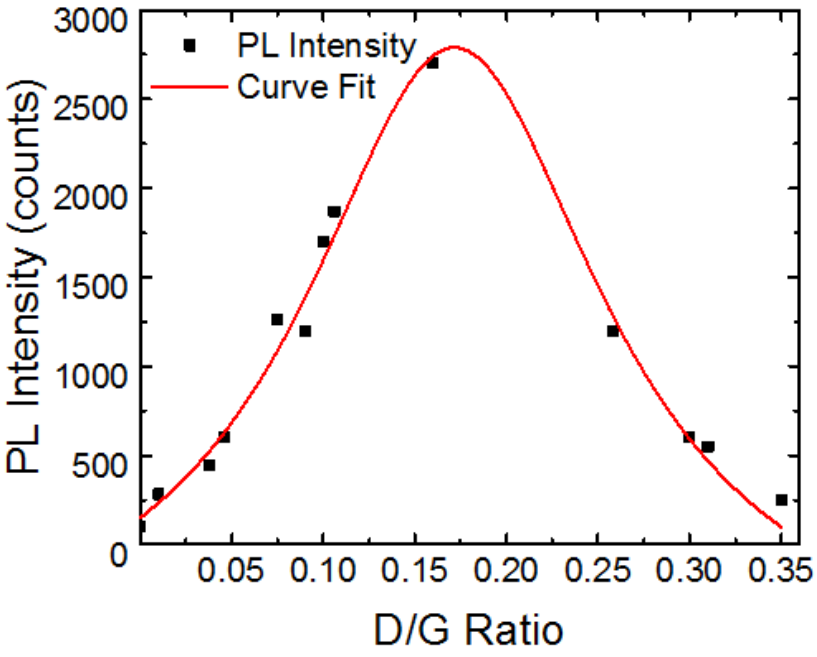

Figure 5. Photoluminescence intensity plotted as a function of the D/G band Raman intensity ratio for 13 different suspended carbon nanotubes. The data here is fit to a Lorentzian function centered around D/G = 0.17.

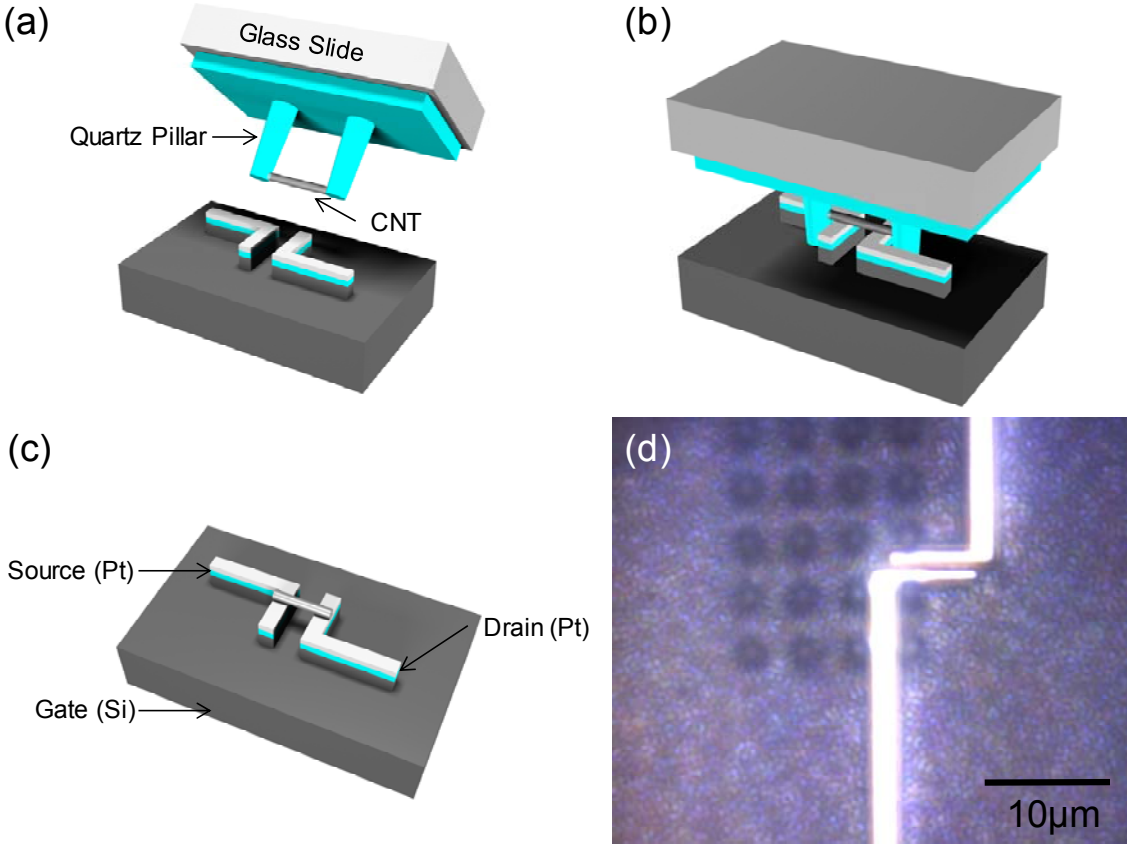

Figure 6. (a-c) Schematic diagrams and (d) optical microscope image of the flip-chip transfer process.

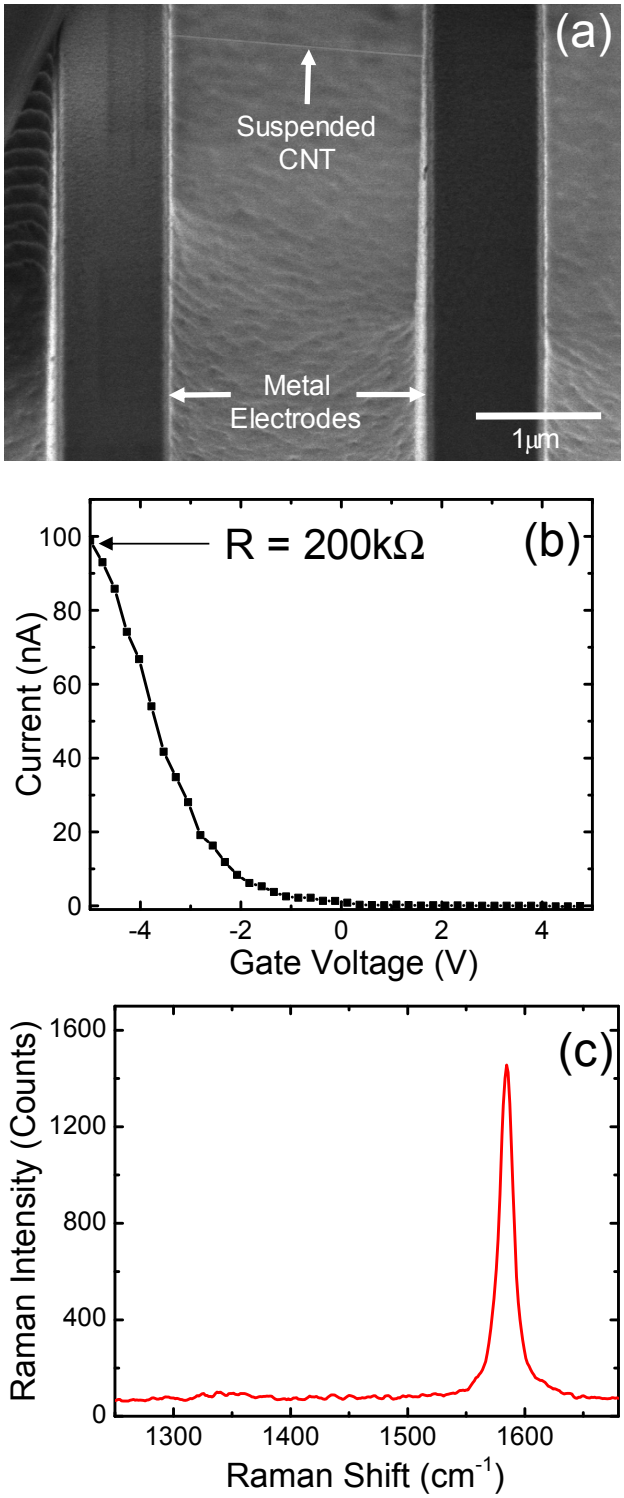

Figure 7. (a) SEM image, (b) current-voltage characteristics, and (c) Raman spectrum of a CNT that was successfully transferred to metal electrodes.

References

[1] Y. M. Piao, B. Meany, L. R. Powell, N. Valley, H. Kwon, G. C. Schatz, Y. H. Wang, Brightening of Carbon Nanotube Photoluminescence through the Incorporation of sp(3) Defects. Nat. Chem. 5, 840-845 (2013).

[2] M. S. Hofmann, J. T. Gluckert, J. Noe, C. Bourjau, R. Dehmel, A. Hogele, Bright Long-lived and Coherent Excitons in Carbon Nanotube Quantum Dots. Nat. Nanotechnol. 8, 502-505 (2013).

[3] I. Sarpkaya, Z. Y. Zhang, W. Walden-Newman, X. S. Wang, J. Hone, C. W. Wong, S. Strauf, Prolonged Spontaneous Emission and Dephasing of Localized Excitons in Air-bridged Carbon Nanotubes. Nat. Commun. 4 (2013).

[4] F. Vialla, Y. Chassagneux, R. Ferreira, C. Roquelet, C. Diederichs, G. Cassabois, P. Roussignol, J. S. Lauret, C. Voisin, Unifying the Low-Temperature Photoluminescence Spectra of Carbon Nanotubes: The Role of Acoustic Phonon Confinement. Phys. Rev. Lett. 113 (2014).

[5] H. Y. Nan, Z. L. Wang, W. H. Wang, Z. Liang, Y. Lu, Q. Chen, D. W. He, P. H. Tan, F. Miao, X. R. Wang, J. L. Wang, Z. H. Ni, Strong Photoluminescence Enhancement of MoS2 through Defect Engineering and Oxygen Bonding, ACS Nano 8, 5738-5745 (2014).

[6] S. Tongay, J. Suh, C. Ataca, W. Fan, A. Luce, J. S. Kang, J. Liu, C. Ko, R. Raghunathanan, J. Zhou, F. Ogletree, J. B. Li, J. C. Grossman, J. Q. Wu, Defects Activated Photoluminescence in Two-dimensional Semiconductors: Interplay between Bound, Charged, and Free excitons, Sci. Rep. 3 (2013).

[7] H. Harutyunyan, T. Gokus, A. A. Green, M. C. Hersam, M. Allegrini, A. Hartschuh, Defect-induced Photoluminescence from Dark Excitonic States in Individual Single-Walled Carbon Nanotubes, Nano Lett. 9, 2010-2014 (2009).

[8] Y. M. He, G. Clark, J. R. Schaibley, Y. He, M. C. Chen, Y. J. Wei, X. Ding, Q. Zhang, W. Yao, X. D. Xu, C. Y. Lu, J. W. Pan, Single Quantum Emitters in Monolayer Semiconductors, Nat. Nanotechnol. 10, 497-502 (2015).

[9] C. Chakraborty, L. Kinnischtzke, K. M. Goodfellow, R. Beams, A. N. Vamivakas, Voltage-controlled Quantum Light from an Atomically Thin Semiconductor, Nat. Nanotechnol. 10, 507-U538 (2015).

[10] A. Srivastava, M. Sidler, A. V. Allain, D. S. Lembke, A. Kis, A. Imamoglu, Optically Active Quantum Dots in Monolayer WSe2, Nat. Nanotechnol. 10, 491-496 (2015).

[11] M. Koperski, K. Nogajewski, A. Arora, V. Cherkez, P. Mallet, J. Y. Veuillen, J. Marcus, P. Kossacki, M. Potemski, Single Photon Emitters in Exfoliated WSe2 Structures, Nat. Nanotechnol. 10, 503-506 (2015).

[12] X. Ma, L. Adamska, H. Yamaguchi, S. E. Yalcin, S. Tretiak, S. K. Doorn, H. Htoon, Electronic Structure and Chemical Nature of Oxygen Dopant States in Carbon Nanotubes, ACS Nano 8, 10782-10789 (2014).

[13] S. Ghosh, S. M. Bachilo, R. A. Simonette, K. M. Beckingham, R. B. Weisman, Oxygen Doping Modifies Near-Infrared Band Gaps in Fluorescent Single-Walled Carbon Nanotubes, Science 330, 1656-1659 (2010).

[14] Y. Miyauchi, M. Iwamura, S. Mouri, T. Kawazoe, M. Ohtsu, K. Matsuda, Brightening of Excitons in Carbon Nanotubes on Dimensionality Modification, Nat. Photonics 7, 715-719 (2013).

[15] X. D. Ma, N. F. Hartmann, J. K. S. Baldwin, S. K. Doorn, H. Htoon, Room-temperature Single-photon Generation from Solitary Dopants of Carbon Nanotubes, Nat. Nanotechnol. 10, 671-675 (2015).
[16] J. Chen, V. Perebeinos, M. Freitag, J. Tsang, Q. Fu, J. Liu, P. Avouris, Bright Infrared Emission from Electrically Induced Excitons in Carbon Nanotubes, Science 310, 1171-1174 (2005).
[17] E. Adam, C. M. Aguirre, L. Marty, B. C. St-Antoine, F. Meunier, P. Desjardins, D. Menard, R. Martel, Electroluminescence from Single-wall Carbon Nanotube Network Transistors, Nano Lett. 8, 2351-2355 (2008).
[18] M. Freitag, V. Perebeinos, J. Chen, A. Stein, J. C. Tsang, J. A. Misewich, R. Martel, P. Avouris, Hot Carrier Electroluminescence from a Single Carbon Nanotube, Nano Lett. 4, 1063-1066 (2004).
[19] S. Khasminskaya, F. Pyatkov, K. Slowik, S. Ferrari, O. Kahl, V. Kovalyuk, P. Rath, A. Vetter, F. Hennrich, M. M. Kappes, G. Gol'tsman, A. Korneev, C. Rockstuhl, R. Krupke, W. H. P. Pernice, Fully Integrated Quantum Photonic Circuit with an Electrically Driven Light Source, Nat. Photonics 10, 727 (2016).
[20] L. Marty, E. Adam, L. Albert, R. Doyon, D. Menard, R. Martel, Exciton Formation and Annihilation during 1D Impact Excitation of Carbon Nanotubes, Phys. Rev. Lett. 96 (2006).
[21] M. S. Dresselhaus, A. Jorio, A. G. Souza, R. Saito, Defect Characterization in Graphene and Carbon Nanotubes Using Raman Spectroscopy, Philos. Trans. Royal Soc. A-Math. Phys. Eng. Sci. 368, 5355-5377 (2010).
[22] M. S. Dresselhaus, G. Dresselhaus, R. Saito, A. Jorio, Raman Spectroscopy of Carbon Nanotubes, Phys. Rep. 409, 47-99 (2005).
[23] C. C. Chang, C. C. Chen, W. H. Hung, I. K. Hsu, M. A. Pimenta, S. B. Cronin, Strain-induced D Band Observed in Carbon Nanotubes, Nano Research 5, 854-862 (2012).
[24] M. R. Amer, S. W. Chang, S. B. Cronin, Competing Photocurrent Mechanisms in Quasi-Metallic Carbon Nanotube pn Devices, Small 11, 3119-3123 (2015).
[25] S. W. Chang, J. Theiss, J. Hazra, M. Aykol, R. Kapadia, S. B. Cronin, Photocurrent Spectroscopy of Exciton and Free Particle Optical Transitions in Suspended Carbon Nanotube pn-junctions, Appl. Phys. Lett. 107, 053107 (2015).
[26] See Supplemental Material at for the spatial profile of the electroluminescence intensity and the plot of current vs. bias voltage from a blank chip.